

Production measurements of heavy quarks in pp collisions at $\sqrt{s} = 13$ TeV with the ALICE detector

Tebogo Joyce Shaba, for the ALICE Collaboration
North-West University, South Africa
iThemba LABS, Sommerset West, Western Cape

E-mail: tebogojoyce.shaba@cern.ch

Abstract. Heavy-flavour production measurements in pp collisions are important tools to test theoretical models based on perturbative quantum chromodynamics (pQCD) and to investigate the heavy-quark hadronization mechanisms. In ALICE, heavy quarks are measured via the hadronic and electronic decay channels at central rapidity ($-0.9 < y < 0.9$) and via the muon decay channels at forward rapidity ($-4 < y < -2.5$).

In this contribution, the production cross-section measurements via the leptonic decay of heavy-flavour hadrons are presented and compared to pQCD theoretical calculations. The latest measurements of D^0 , D^+ , D^{*+} , D_s^+ mesons whose hadronic decays into charged are fully reconstructed together with the measurements of Λ_c^+ , $\Xi_c^{0,+}$, $\Sigma_c^{0,++}$ and Ω_c^0 baryons, performed with the ALICE detector at midrapidity in pp collisions at $\sqrt{s} = 13$ TeV, are also presented. Measurements of charm-baryon production are crucial to study the charm-quark hadronization mechanisms in a partonic rich environment like the one produced in pp collisions at LHC energies.

1. Introduction

Heavy-flavours (charm and beauty) are abundantly produced at the LHC [1] in the early stages of hadronic collisions via hard parton-parton scattering processes and therefore experience the full evolution of the system. The measurement of heavy flavours in pp collisions can be used to test pQCD calculations. In addition, these measurements provide an essential baseline for the studies of nuclear (p-Pb and Pb-Pb) collisions. Heavy flavour production in nuclear collisions is modified by cold nuclear matter effects (CNM) such as shadowing and energy loss [2, 3]. The knowledge of these effects is fundamental for understanding the interactions of heavy quarks with the deconfined medium formed in heavy-ion collisions where the modified transverse momentum (p_T) distribution can be used to infer the effect of the interactions with the QGP. Heavy-quark production is experimentally accessible through the measurement of heavy-flavour hadrons and their decay products.

At the LHC, ALICE [4] comprises several subdetectors, which are used for the measurement of charged hadrons, charged leptons and photons, including forward muon spectrometer which measures muons. The L3 solenoid magnet provides a field of 0.5 T to the central barrel detectors covering the rapidity $-0.9 < y < 0.9$. The Silicon Pixel Detector (SPD), as part of the inner tracking system, is used for the determination of the interaction vertex as well as the

measurement of charged-particle multiplicity. Particle-identification information is given by the Time Of Flight (TOF) and the Time Projection Chamber (TPC). Two arrays of scintillator detectors (V0A and V0C), placed on both sides of the interaction point provide centrality in Pb–Pb collisions as well as trigger information and beam-gas background suppression. They are also used for multiplicity determination. The Transition Radiation Detector (TRD), is used for the electron identification through the ionization energy and the Electromagnetic Calorimeter (EMCal) that is the last detector before the magnet is used to improve ALICE capacity in p_T reconstruction of jets, direct photons and electrons from heavy flavor decay. The forward muon spectrometer covers the rapidity range $-4 < y < -2.5$. It consists of a composite absorber, a dipole magnet, five tracking stations, a muon filter and two trigger stations. The absorber reduces background muons mainly from the decays of pions and kaons. The dipole magnet provides a horizontal magnetic field perpendicular to the beam axis and is used for charge and momentum determination. The tracking stations are used to determine the trajectories of the muons traversing the detector. The muon filter is mounted in front of the trigger stations and filters out all particles with momentum $p < 4$ GeV/c. The trigger stations are used for muon identification and triggering.

The reconstruction of charm baryons and mesons is done via their hadronic decay channels. Table 1 below shows the decay channels and their branching ratios (BR)

Charm mesons	Charm Baryons
$D^0 \rightarrow K^- \pi^+$ (3.88±0.05 %)	$\Lambda_c^+ \rightarrow K_c^+ p$ (1.59±0.08%)
$D^+ \rightarrow K^- \pi^+ \pi^+$ (9.13±0.19 %)	$\Xi_c^0 \rightarrow \Xi^- \pi^+$ (1.43±0.32 %)
$D^{*+} \rightarrow D^0 \pi^+$ (67.7±0.05 %)	$\Sigma_c^{0,++} \rightarrow \Lambda_c^+ \pi^-$ ($\approx 100\%$)
$D_s^+ \rightarrow K^- K^+ \pi^+$ ($\approx 5.39\%$)	$\Omega_c^0 \rightarrow \Omega^- \pi^+$ (0.51±2.19 %)

Table 1. The hadronic decay modes of charm mesons and charm baryons exploited by ALICE with in parenthesis the respective BR.

2. Results

2.1. Charm baryon production cross sections

Figure 1a and 1b [5] respectively, shows the p_T -differential cross section of prompt D^0 and charm baryons: Λ_c^+ , $\Sigma_c^{0,++}$ (left), and prompt-charm-hadron cross-section ratio of Λ_c/D^0 (right) in pp collisions at $\sqrt{s} = 13$ TeV. The baryon-to-meson yield ratios are taken into consideration to probe different hadronisation mechanisms. The baryon-to-meson yield ratios are higher in pp collisions at LHC energies than in e^+e^- collisions, suggesting that charm hadronisation occurs via different processes in the two collision systems. The Λ_c/D^0 ratio decreases with increasing p_T and has a strong enhancement for $p_T < 10$ GeV/c. The values measured in pp collisions at $\sqrt{s} = 13$ TeV are compatible, within uncertainties, with those measured at $\sqrt{s} = 5$ TeV.

2.2. Heavy charm baryons $\Sigma_c^{0,++}$, Ξ_c^+

In Figure 2, the $\Sigma_c^{0,++}/D^0$ (left) [5] ratios shows a remarkable difference between the pp and e^+e^- collisions by a factor of approximately 10. In Figure 2, the data are described well by the models, except for PYTHIA8 Monash Tune [8]. The baryon-to-meson ratio (right) [6] increases towards low p_T up to a value of approximately 0.3, while PYTHIA8 Monash, PYTHIA8 CR

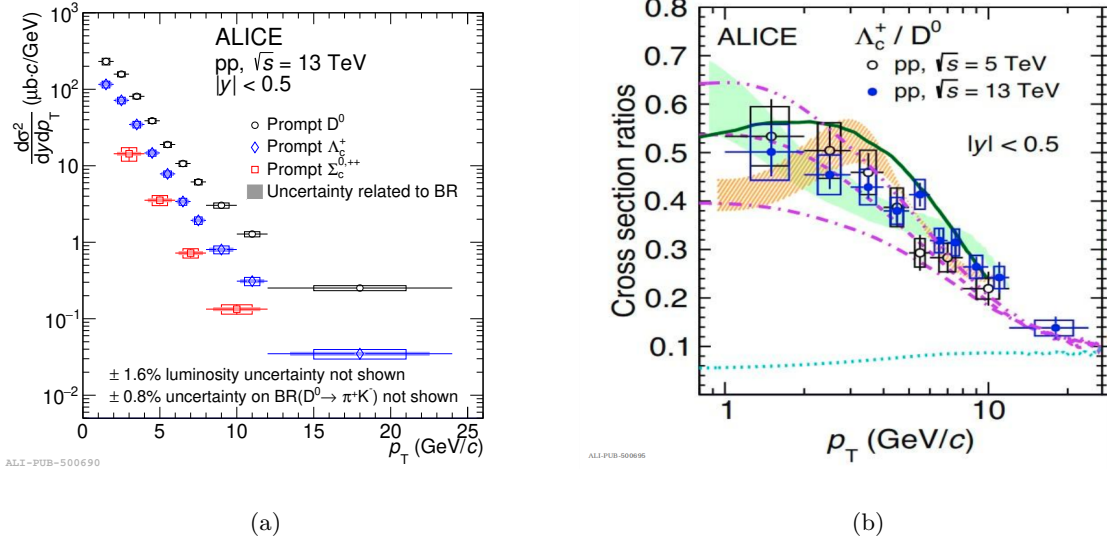


Figure 1. p_T -differential cross sections of prompt D^0 , Λ_c , and $\Sigma_c^{0,++}$ (left) and prompt-charm-hadron cross-section ratios (right) at $\sqrt{s} = 13$ TeV compared with data from pp collisions at $\sqrt{s} = 5$ TeV [5].

Tune [9], SHM+RQM [10] and QCM [11] significantly underestimate the ratios. The Catania model [12] describes better the ratios in the measured p_T interval.

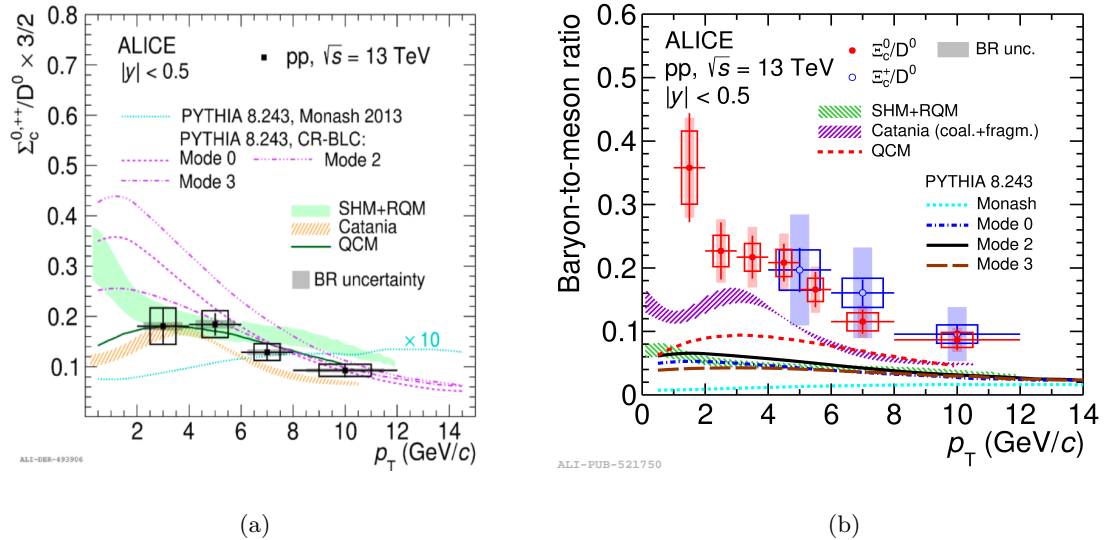


Figure 2. The prompt-charm-hadron cross section ratios (right) for $\Sigma_c^{0,++}/D^0$ (left) [5] and Ξ_c^0/D^0 and Ξ_c^+/D^0 ratio (right) [6] as a function of p_T in pp collisions at $\sqrt{s} = 13$ TeV

2.3. Heavy charm baryons Ω_c^0

In Figure 3 [7], the measurement of Ω_c^0 is compared with model predictions of the PYTHIA 8 Monash tune and with CR (colour reconnections) beyond the leading-colour approximation [9], which are multiplied by a theoretical BR ($\Omega_c^0 \rightarrow \Omega^+ \pi^-$). The cross section from the CR-BLC tune [13] is larger than the one from the Monash tune by a factor varying between 9 and 25 depending on p_T .

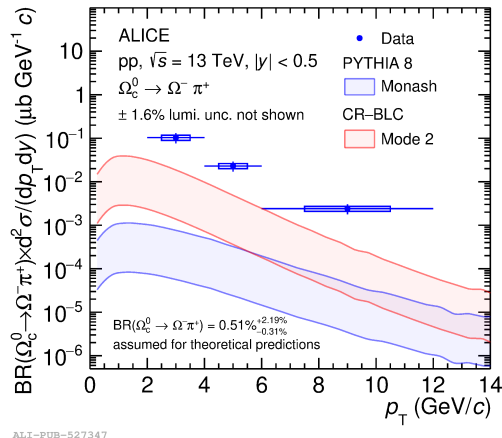


Figure 3. The p_T -differential production cross section of inclusive Ω_c^0 baryons multiplied by the branching ratio into $\Omega^+ \pi^-$ in pp collisions at $\sqrt{s} = 13$ TeV [7].

3. Conclusion

PYTHIA 8 Monash, which adopts fragmentation functions constrained in e^+e^- and e^+p collisions, significantly underestimate the baryon-to-meson productions, while models with an augmented formation of baryons (PYTHIA 8 CR tunes, SHM+RQM, Catania) are closer to the data and can describe Λ_c and Σ_c , for the strange charm baryons (Ω_c , Ξ_c). All the models underestimate the data, with the Catania model providing the closest agreement. The non-prompt Λ_c^+ / D^0 provides indirect access to the beauty fragmentation. The p_T trend of prompt and non-prompt Λ_c^+ / D^0 is similar.

References

- [1] ALICE Collaboration. *Journal of Instrumentation*, 3:S08001, 2008.
- [2] S. Gavin and J. Milana. *Physics Review Letters* 68 (1992) 1834.
- [3] S. Brodsky and P Hoyer. *Physics Letters B* 298 (1993) 165.
- [4] ALICE Collaboration. *International Journal of Modern Physics A* 20:1430044, 2014.
- [5] ALICE Collaboration. *Physical review letters* 012001 (2022) 128.
- [6] ALICE Collaboration. *Physical review letters* 272001 (2021) 127.
- [7] ALICE Collaboration. *arXiv preprint arXiv:2205.13993* (2022).
- [8] T. Sjöstrand, S. Ask, J.R. Christiansen, R. Corke, N. Desai, P. Ilten, S. Mrenna, S. Prestel, C.O. Rasmussen and P.Z. Skands. *Computer physics communications* 159–177 (2015) 191.
- [9] R. Christiansen, R. Jesper P.Z. Skands and Z. Peter. *Journal of High Energy Physics* 1–52 (2015) 2015.
- [10] M. He, R.J. Fries and R. Rapp. *Physics Letters B* 1–24 (2012) 2012.
- [11] J. Song, H. Li and F. Shao. *The European Physical Journal C* 1–8 (2018) 78.
- [12] S. Plumari, V. Minissale, S.K Das, G. Coci and V. Greco. *The European Physical Journal C* 1–13 (2018) 78.
- [13] P. Skands, S. Carrazza and J.Rojos. *The European Physical Journal C* 1–39 (2014) 74.